Vertical wavenumber spectral characteristics of temperature in the stratosphere-mesosphere over tropical and subtropical regions

Priyanka Ghosh* and Som Sharma

Physical Research Laboratory, Ahmedabad - 380009, India

**Corresponding author*

E-mail address: priyankag@prl.res.in, iam.priyankaghosh@gmail.com

Abstract

The vertical wavenumber spectra over tropical location, Gadanki (13.5º N, 79.2º E) and sub-tropical location, Mt. Abu (24.5º N, 72.7º E) is studied using the temperature measurements from ground based Rayleigh Lidar and space borne satellite observations. The slope values are lesser over Gadanki than at Mt. Abu for almost all the altitudes except for 40-50 km where it is nearly same and 60-70 km exhibiting opposite nature. Unusual spectral slope of -6.97 (Mt. Abu) and -0.09 (Gadanki) is seen at the altitude of 40-50 km in satellite temperature. Characteristics of wave oscillations perceived over both the stations are described.

Key words: lidar; vertical wavenumber spectra; spectral slope; wave oscillation

1. Introduction

Atmospheric gravity waves (GWs) are abundantly generated in the earth's lower atmosphere which affects the energy and momentum budget in the middle and upper atmosphere by regulating and altering the thermodynamical structure of the atmosphere significantly (Fritts and Alexander, 2003). Therefore, it is essential to have a thorough knowledge of the atmosphere GWs characteristics for better understanding of the global mesospheric dynamics. When the GWs proliferate vertically upward, their amplitude intensifies exponentially due to decrease in atmospheric density resulting in convective or dynamic instability in the surrounding area. Therefore, the GWs releases energy to maintain overall stability, during upward propagation, while the power of wavenumber spectra and the spectral slope becomes saturated. VanZandt (1982) coined the purported 'universal' wavenumber spectra referring to the independent behavior of the frequency, horizontal and vertical wavenumber spectra of horizontal wind and temperature fluctuations (specifically in the higher wavenumber region) irrespective of altitude, season and geographical location. Numerous studies have been show similarities or dissimilarities in observation with VanZandt (1982) proposition using ground-based and satellite-borne instruments (e.g., Eckermann, 1995; Ghosh et al., 2018; Larsen et al., 1986; Smith et al., 1987; Zhang et al., 2017a,b and references therein). Gardner et al., (1993) derived a model of vertical wavenumber (VWN) spectra of GWs, for atmospheric density and velocity fluctuations, where the spectral slopes are '2', '-3' and '-5/3' for unsaturated, saturated and turbulence region respectively. Recently, Ghosh et al., (2018) found the saturated spectral slope of vertical wind, observed using mesosphere stratosphere troposphere (MST) radar over a tropical location Gadanki (13.5º N, 79.2º E), to be ~-6, ~-9 and ~-12 in some cases. The foremost purpose of this paper is to investigate the VWN spectral characteristics over a tropical location Gadanki (13.5º N, 79.2º E) and a sub-tropical location Mt. Abu (24.5º N, 72.7º E). For this work, simultaneous observations of ground-based Rayleigh lidar at both the locations are used along with Sounding of the Atmosphere using Broadband Emission Radiometry (SABER) temperature measurements onboard Thermosphere Ionosphere Mesosphere Energetics and Dynamics (TIMED) satellite.

2. Data and instrumentation

Rayleigh lidar at Mt. Abu (24.5º N, 72.7º E) was installed by Physical Research Laboratory (PRL) and at Gadanki (13.5º N, 79.2º E) by National Atmospheric Research Laboratory (NARL) for middle atmospheric temperature measurements. The details of both the lidar systems are available in Sharma et al., (2017) and Sivakumar et al., (2003). For the present study, the lidar temperature covers the altitude of 33-70 km divided into 33-40 km, 40-50 km, 50-60 km and 60-70 km over Mt. Abu (during 14-21 March 2004) and 30-66 km divided into 30-40 km, 40-50 km, 50-60 km and 60-66 km over Gadanki (during 19-26 March 2004). SABER is one of National Aeronautics and Space Administration's TIMED satellite with latitude coverage of 52º N to 83º S (all through the north observing mode for nearly 60 days) or 52º S to 83º N (in the south observing mode) (Russell III et al., 1999). Therefore, the TIMED satellite can continuously access the latitudes 52º S to 52º N (Mertens, 2004; Mertens et al., 2001). The temperature measurements from SABER instrument is obtained for the longitude grid of 23-25º N (12-14º N) and longitude grid of 70-73º E (78-81º E) over Mt. Abu (Gadanki) during the time period of 20:00 UT to 21:30 UTC respectively. Earlier studies reported that the spectra are 'red' at the higher wavenumbers for most of the atmospheric variables (Blackman and Turkey, 2009; Percival and Walden, 1993). Therefore, various methods are used in the past to overcome or reduce spectral leakage. To conserve the 'spectral density' at small wavenumbers, it is found that the 'prewhitening with first differences' methodology is very efficient (Nastrom and VanZandt, 2001; Tsuda et al., 1989). The daily temperature profiles are normalized ($T'/\bar{T}$, where T' is the temperature fluctuation and $\bar{T}$ is the mean temperature) (Allen and Vincent, 1995; Guharay and Sekar, 2011; Nastrom et al., 1997; Tsuda and Hocke, 2002; Yan et al., 2019) and subjected to spectral analysis using Fast Fourier Transform (FFT) (after 'prewhitening/postcoloring' techniques) to acquire the proliferation characteristics of dominant wave oscillations and the VWN spectral slope values. The normalized daily temperature data is 'prewhitened' by removing the 'first difference' of the residuals (X_q) using the methodology suggested by Nastrom and VanZandt, (2001) as follows:

$$\overline{X_q} = X_q - \alpha X_{q-1} \qquad (1)$$

Here, the value of α is 1 (Dewan and Grossbard, 2000; Nastrom and VanZandt, 2001; and references therein for more details of 'prewhitening').

Using Fast Fourier Transform (FFT) analysis, the spectral amplitude of the 'prewhitened' data is determined. The 'postcolored' spectra (F_{PWPC}) is obtained using the following equation (Nastrom and VanZandt, 2001):

$$F_{PWPC}(m_{r,j}) = \frac{F_{PW}(m_{r,j})}{2[1-\cos(2\pi j/M)]} \qquad (2)$$

where $m_{r,j} \rightarrow j$ th wavenumber in radians/meter ($m = m_r/2\pi$) in cycles/meter, and M → total number of data points.

In order to show the difference in spectral slope before 'prewhitening/postcoloring', the power spectral density (PSD) obtained using Fast Fourier Transform (FFT) on the normalized temperature data without 'prewhitening/postcoloring' is also calculated and both the slope values (where 'Slope 1' indicates slope values without 'prewhitening/postcoloring' and 'Slope 2' denotes slope values after inclusion of 'prewhitening/postcoloring') are tabulated in **Table 1** and also plotted in all the figures (**Figure 1-9**). To measure the accuracy of VWN spectral slopes, co-efficient of determination (R^2) of the spectral slopes using lidar and SABER/TIMED observation [with and without Pre-whitening and Post-Coloring (PWPC)] over Mount Abu (24.5º N, 72.7º E) and Gadanki (13.5º N, 79.2º E) for the individual height regions covering the whole range of 30-

70 km is calculated (**Table 2 and 3**; where **Table 2** is based on lidar and **Table 3** depicts the SABER/TIMED observation on the nearest possible day over both stations depending on data availability). The standard deviation of R^2 values is indicated with '±' sign.

3. Results and discussion

For the PSD calculation, nightly mean data has been used and the selected nights have more than 2-3 hours observation on each day (depending upon local weather conditions). Each profile is of 5 or 10 minutes and all the profiles collected in a single night are integrated to improve the signal to noise ratio. Altitude profile of VWN spectra using lidar temperature observation over Mt. Abu during 14-17 March 2004 shown in **Figure 1** where the x-axis denotes the natural logarithm of wavenumber (cycles/km) and y-axis denotes the natural logarithm of PSD (K^2/wavenumber). It is to be noted that all the slope values discussed here are approximate. It is observed that the spectral slope is more negative in the altitude range of 40-50 km (fluctuating between -2.67 to -2.82) and 60-70 km (fluctuating between -2.58 to -2.72) except for 16 March where the slope is most negative (-2.88) at the height of 56-60 km. In case of the altitude profile of VWN spectra during 18-21 March 2004 (**Figure 2**), similar pattern is observed with most negative slopes in the elevations of 40-50 km (between -2.5 to -2.94) and 60-70 km (between -2.68 to -2.79) except for 18 March which shows the spectral slope of -2.79 at the height of 50-60 km. Ghosh et al., (2018) suggested that the tropopause may act as the source of new gravity waves resulting in positive VWN spectral slope value. Since the stratopause exists in the altitude of 45-50 km, the more negative slope at that elevation can be contributed to the presence of stratopause which is a transition zone of atmosphere. It is to be also taken into account that the station Mt. Abu is located at an elevation of about 1.7 km from the mean sea level which may also add up to the changes in spectral slope due to the presence of terrain generated gravity waves.

In case of the altitude profile of VWN spectra over Gadanki during 19-22 March 2004 (**Figure 3**), it is perceived that the spectral slope is more negative at the heights of 30-40 km (ranging between -2.71 to -3.01) and 40-50 km (between -2.94 to -3.25) in contrast to the observations over Mt. Abu. Although the spectral slope values in the elevations of 50-60 km are more negative than those of 60-66 km, still they less negative than the ones in 30-40 km and 40-50 km heights. Similar pattern is detected for the VWN spectral slope values in **Figure 4** except for 26 March 2004 where the most negative slopes occur at 40-50 km and 50-60 km. Guharay and Sekar, (2011) used

Rayleigh lidar observations over Gadanki operated in cloud free nights on a systematic manner with more than 4 hours of unswerving observation to investigate GWs of periodicities less than 4 hours (during March 1998 – December 2008). They reported that the spectral slope in the upper stratosphere (35-50 km) is considerably higher (~ -2.83) and nearly corresponds to the theoretical magnitude of spectral slope obtained than those observed in the mesospheric (50-72 km) heights (~ -2.53). They also suggested that this may affect the mesosphere such that it becomes more susceptible to maintain 'nonlinear wave interaction processes' rather than 'individual wave packet propagation'. In the present case, the spectral slope values over Mt. Abu are below '-3' ranging from -2.14 to -2.93 (without 'prewhitening/postcoloring') and -2.71 to -2.97 (with 'prewhitening/postcoloring') (during 14-17 March 2004) but for Gadanki it ranges from -1.78 to -3.25 (without 'prewhitening/postcoloring') and -2.39 to -3.13 (with 'prewhitening/postcoloring') (during 19-26 March 2004). The higher spectral slope value of -1.78 or -2.39 and -2.90 (without or with 'prewhitening/postcoloring') over Gadanki corresponds to the altitude of 60-66 km and the lower values of -3.25 or -3.13 (without or with 'prewhitening/postcoloring') is seen at 40-50 km. In this scenario, the mesospheric spectral slopes are much lower than the upper stratospheric slopes which is not observed by Guharay and Sekar, (2011). In general, the spectral slope values are below the theoretical saturated slope value of '-3' (except August and October) (Guharay and Sekar, 2011) which is mostly similar to our observation over both the tropical and sub-tropical station of Gadanki (except at few altitudes) and Mt. Abu, respectively (**Table 1**).

The VWN spectral slope values on the common operational days (19 March 2004, 20 March 2004 and 21 March 2004) over both Gadanki and Mt. Abu are compared in **Figure 5**, **Figure 6** and **Figure 7** respectively to have an insight of the spectral slope variation with height. The slope values are more negative over Gadanki (tropical station) than Mt. Abu (sub-tropical station) for all the altitudes except for 40-50 km where it is same and 60-70 km where slope value over Mt. Abu is lesser than Gadanki (**Figure 5**). On 21 March 2004, the spectral slopes are more negative over Gadanki than Mt. Abu except for the height of 50-60 km and 60-70 km (**Figure 6**). In **Figure 7**, similar features resembling **Figure 5** is observed where the slope values are nearly same at 40-50 km and lesser over Mt. Abu than Gadanki at 60-70 km. Guharay et al., (2010) using radiosonde measurements over Gadanki reported the mean spectral slope to be -2.83 at the heights of 18–30 km (in the lower stratosphere). Our observations are similar to that of Guharay et al., (2010) except for the fact in some instances more negative slope values in the upper stratosphere (lesser than the theoretical saturated spectral slope value of '-3' is seen). Yu and Yi, (2008) took simultaneous observation from Raman and Rayleigh lidar (covering 4-60 km) over Wuhan, China (30.5º N, 114.4º E) and found the spectral slope value to be nearly '-3'. Sato and Yamada, (2004) also reported the saturated slope value over Shigaraki, Japan (35º N, 136º E) around the theoretical value of '-3' and presumed that the probable effect of 'large-scale wind shear' on VWN spectra. Tsuda et al., (1991) observed the spectral slope in the lower stratosphere (18.5-25 km) ranging between -2.9 to -3.2 in winter months while it ranges between -2.2 to -2.4 during the summer over Shigaraki, Japan (35º N, 136º E) using campaign radiosonde soundings. Allen and Vincent, (1995) used radiosonde data over 18 stations in Australia and Antarctica (covering the latitudinal range of 12º S - 68º S and longitudinal range of 78º E - 159º E) and found the mean spectral slope to be ~ -2.5 (lower stratosphere). Over Andenes, Norway (69.3ºN), Wu and Widdel, (1989) reported the slope value (logarithmic) of ~ -3.0 ± 0.2 at the altitudes of 80-95 km using horizontal wind measurements.

The spectral slope obtained using ground-based Rayleigh lidar observations are compared with space borne SABER satellite measurements. The altitude profile of VWN spectra obtained from SABER temperature is plotted over Gadanki and Mt. Abu (**Figure 8** and **Figure 9**). **Figure 8** displays the VWN spectra on 18 March over Mt. Abu and 19 March over Gadanki respectively. The slopes over Gadanki are more negative than Mt. Abu (similar to **Figures 5-7**) except for the altitude of 40-50 km where the slope value is -6.97 (for Mt. Abu) and -0.09 (for Gadanki). The presence of stratopause at that altitude along with the location of Mt. Abu at about 1.7 km above mean sea-level which jointly may result in such distinct observation. Yan et al., (2019) found the spectral slope ranging from -1.6 to -3.0 whereby mostly the slope values are less negative than the theoretical value of '-3' using Constellation Observing System for Meteorology, Ionosphere and Climate (COSMIC) temperature data (during January 2007 to February 2014) revealing a 'quasi-biennial cycle' at low latitudes, 'annual cycle' at middle and high latitudes, and 'semi-annual cycle' at boreal high latitudes. Further, they also provided evidence that the spectral slope barely has any longitudinal variation and strongly proposed the slope to be of 'universal nature' where the wave propagation processes (for example, 'wave-wave' or 'wave-background flow' interaction) plays a dominant role rather than the GW sources. Zhang et al., (2017a) used 11 years of radiosonde data (1998-2008) over 92 stations of United States (in the Northern Hemisphere) and reported that the 'vertical wind spectrum' is less negative than the 'horizontal wind spectrum' over a wide latitudinal region, with slopes varying between -1.1 to -0.2 in the troposphere and -0.6 to 0.1 in the lower stratosphere. Although our observations are not exactly similar to that of Yan et al., (2019) and Zhang et al., (2017a), their results support the shallow VWN spectral slope value of -1.78 or -2.90 (lidar observation) and -0.09 or -1.53 (without or with 'prewhitening/postcoloring') (SABER/TIMED observation) over Gadanki in the present study. However, the much negative slope of -6.97 (-4.97) (without or with 'prewhitening/postcoloring') observed with SABER/TIMED observations over Mt. Abu at the altitudes of 40-50 km can only be explained by the assumptions that this can be due to the proximity of stratopause which is a 'transition zone' between two atmospheric layers presumably interfering with the generation and breaking of waves (at present and it need to be investigated further in future). The ambiguity could not be due to the linear fit of five points because in that case all the other height regions with similar number of data points also would have shown some discrepancy. Since it is only seen at one altitude range over both the tropical and sub-tropical stations, it need to be looked into in detail in future with more simultaneous observations. Ghosh et al., (2018) found the presence of positive slope (at the altitudes of 12-17 km) and concluded that it may be due to the presence of tropopause which may instigate the generation of new GWs. In **Figure 9**, no such discrete slope is observed and it is seen that the slope values are more negative at Gadanki in the altitude range of 40-50 km and 60-70 km and vice-versa. The altitude profile of amplitude and phase of the dominant wave oscillations over Gadanki (during 19-26 March 2004) and Mt. Abu (during 14-21 March 2004) is plotted in **Figure 10**.

The amplitudes of atmospheric gravity wave (GW) increases exponentially due to decrease in atmospheric density as they proliferate from the lower to the higher atmosphere. Throughout their propagation, these GWs divulge energy to the surroundings while their 'power of wavenumber spectra' and 'spectral slope' gets saturated to conserve the overall stability. This resulted in the theory of universal wavenumber spectra with three distinct regions: unsaturated (log-log slope of 2), saturated (log-log slope of -3), and turbulence region (log-log slope of -5/3). Therefore, the GWs oscillation and vertical wavenumber spectral slope are related. If continuous temperature or wind measurements are available, it can be utilized to study the dominant GW oscillations present during the observation period. There have been various studies in past (Ghosh and Ramkumar, 2014; Gong et al., 2018; Ma et al., 2017) which linked some particular wave oscillations (e.g. 2-day, 5-day, 3-day) with the vertical wave number spectral slope or with certain dynamic events like sudden stratospheric warming (SSW), convection, etc. obtained over that particular station. In the present study, continuous nightly mean temperature observations are available for 8 days (where the lidar is run for 2-3 hours) at both the subtropical and tropical locations. This provides an opportunity to see if planetary waves also can be linked with vertical wavenumber spectral slope or not. Therefore, in the present study, we made an attempt to link the vertical wavenumber spectra with the dominant wave oscillations (for e.g., how the amplitude, phase and vertical wavelength varies) over both stations. It is seen that about 4-day, 2.7-day and 2-day oscillations dominant over both the stations during the observation period. One interesting feature is that the 2-day oscillation shows standing nature over Gadanki (tropical station at 375 m elevation surrounded by small terrains) as well as Mt. Abu (sub-tropical station at an elevation of about 1.7 km). The vertical wavelength of about 4-day, 2.7-day and 2-day oscillation calculated from the altitude profile of phase is tabulated in **Table 1**. It is to be noted that the 2-day wave have a single vertical wavelength value throughout the altitude profile owing to its standing nature. The vertical wavelength (km) over Gadanki (Mt. Abu): for 4-day oscillation ranges from 3.52-25.54 (8.37-43.64) km, for 2.7 day oscillation 4.89-17.81 (3.87-16.41) km, and for 2-day oscillation it is 22.19 (29.82) km.

4. Summary and conclusions

The present study describes in detail the VWN spectral slope characteristics over a tropical station of Gadanki and sub-tropical station of Mt. Abu. It is observed that the spectral slopes over Gadanki are more negative in most of the altitudes with some exceptions. This could be due to the fact that over Gadanki, the convectively generated gravity waves play a major role whereas in case of Mt. Abu, mountain generated gravity waves affects the atmosphere in majority. Although more negative slope value than the theoretical saturated slope of '-3' is observed over Gadanki, they are much less than those reported by Ghosh et al., (2018) in the order of ~ -6, ~ -9 and ~ -12. Moreover, in the present case no positive spectral slope is observed indicating wave generation (Ghosh et al., 2018). The spectral slopes observed in the present study depict similar spectral slope nature over Gadanki as reported by earlier studies using radiosonde (Guharay et al., 2010) and Rayleigh lidar (Guharay and Sekar, 2011) over Gadanki. To investigate convection generated gravity wave effect on VWN spectra, further studies need to done with large datasets in future and other instruments (as Rayleigh lidar cannot be operated during cloudy and rainy nights). Our observations even match with the earlier studies made with COSMIC temperature, radiosonde and radio occultation measurements in the mid and high latitudes (Zhang et al., 2017a; Tsuda and Hocke, 2002; Yan et al., 2019). Since lidar observations are made simultaneously over both subtropical and tropical stations during similar period, it gave an opportunity to study planetary wave oscillations over both the locations and how their characteristics vary over each locations. Similar wave oscillations are observed over both the stations with periodicities of about 4-day, 2.7-day and 2-day with comparable vertical wavelength. One interesting feature is that the 2-day wave shows standing nature over both the tropical and sub-tropical locations.

5. Acknowledgement

The present study is supported by Department of Space, Govt. of India. We are thankful to the lidar group members of Physical Research Laboratory (PRL) and National Atmospheric Research Laboratory (NARL) for observational data at Mt. Abu and Gadanki respectively. Priyanka Ghosh thanks Sivakandan Mani for his support. The authors convey their heartfelt gratitude to the anonymous reviewer and editor for their constructive suggestions which enriched the paper.

6. References

Allen, S.J., Vincent, A., 1995. Gravity wave activity in the lower atmosphere: seasonal and latitudinal variations. Journal of Geophysical Research, 100(D1), 1327-1350. https://doi.org/10.1029/94JD02688

Bhatt, H., Sharma, S.K., Trivedi, R., Vats, H.O., 2018. Variability of fractal dimension of solar radio flux. Mon. Not. R. Astron. Soc. 475, 3117–3120. https://doi.org/10.1093/mnras/stx3273

Blackman, R.B., Tukey, J.W., 2009. The Measurement of Power Spectra. Phys. Today 13, 52–54. https://doi.org/10.1063/1.3056826

Dewan, E.M., Grossbard, N., 2000. Power spectral artifacts in published balloon data and implications regarding saturated gravity wave theories. J. Geophys. Res. Atmos. 105, 4667–4683. https://doi.org/10.1029/1999jd901108

Eckermann, S.D., 1995. Effect of background winds on vertical wavenumber spectra of atmospheric gravity waves. J. Geophys. Res. 100, 14097. https://doi.org/10.1029/95JD00987

Fritts, D.C., Alexander, M.J., 2003. Gravity Wave Dynamics and Effects in the Middle Atmosphere. Rev. Geophys. 41, 1–64. https://doi.org/10.1029/2001RG000106

Gardner, C.S., Hostetler, C.A., Franke, S.J., 1993. Gravity wave models for the horizontal wave number spectra of atmospheric velocity and density fluctuations. J. Geophys. Res. 98, 1035–1049. https://doi.org/10.1029/92JD02051

Ghosh, P., Ramkumar, T.K., 2014. Vertical temperature wave number spectra of the Martian lower atmosphere. Atmos. Sci. Lett. https://doi.org/10.1002/asl2.545

Ghosh, P., Ramkumar, T.K., Sharma, S., 2018. Anomalous Behavior of Vertical Wavenumber Spectra Over a Tropical Station of India. Geophysical Research Letters, 45, 12553-12559. https://doi.org/10.1029/2018GL079934

Gong, Y., Li, C., Ma, Z., Zhang, S., Zhou, Q., Huang, C., Huang, K., Li, G., Ning, B., 2018. Study of the Quasi-5-Day Wave in the MLT Region by a Meteor Radar Chain. J. Geophys. Res. Atmos. 123, 9474–9487. https://doi.org/10.1029/2018JD029355

Guharay, A., Sekar, R., 2011. Seasonal characteristics of gravity waves in the middle atmosphere over Gadanki using Rayleigh lidar observations. J. Atmos. Solar-Terrestrial Phys. 73, 1762–1770. https://doi.org/10.1016/j.jastp.2011.04.013

Guharay, A., Venkat Ratnam, M., Nath, D., Dumka, U.C., 2010a. Investigation of saturated gravity waves in the tropical lower atmosphere using radiosonde observations. Radio Sci. 45, 1-14. https://doi.org/10.1029/2010RS004372

Larsen, M.F., Woodman, R.F., Sato, T., Davis, M.K., Larsen, M.F., Woodman, R.F., Sato, T., Davis, M.K., 1986. Power Spectra of Oblique Velocities in the Troposphere and Lower Stratosphere Observed at Arecibo, Puerto Rico. J. Atmos. Sci. 43, 2230–2240. https://doi.org/10.1175/1520-0469(1986)043<2230:PSOOVI>2.0.CO;2

Ma, Z., Gong, Y., Zhang, S., Zhou, Q., Huang, C., Huang, K., Yu, Y., Li, G., Ning, B., Li, C., 2017. Responses of Quasi 2 Day Waves in the MLT Region to the 2013 SSW Revealed by a Meteor Radar Chain. Geophys. Res. Lett. Lett. 44, 9142–9150. https://doi.org/10.1002/2017GL074597

Mertens, C.J., 2004. SABER observations of mesospheric temperatures and comparisons with falling sphere measurements taken during the 2002 summer MaCWAVE campaign. Geophys. Res. Lett. 31, L03105. https://doi.org/10.1029/2003GL018605

Mertens, C.J., Mlynczak, M.G., López-Puertas, M., Wintersteiner, P.P., Picard, R.H., Winick, J.R., Gordley, L.L., Russell, J.M., 2001. Retrieval of mesospheric and lower thermospheric kinetic temperature from measurements of CO2 15 υm earth limb emission under non-LTE conditions. Geophys. Res. Lett. 28, 1391–1394. https://doi.org/10.1029/2000GL012189

Nastrom, G.D., VanZandt, T.E., 2001. Seasonal variability of the observed vertical wave number spectra of wind and temperature and the effects of prewhitening. J. Geophys. Res. Atmos. 106(D13), 14369–14375. https://doi.org/10.1029/2001JD900163

Nastrom, G.D., VanZandt, T.E. and Warnock, J.M. (1997), Vertical wave number spectra of wind and temperature from high-resolution balloon soundings over Illinois. Journal of Geophysical Research, 102(D6), 6685-6701.

Percival, Donald B. and Walden, A.T., 1993. Spectral Analysis For Physical Applications Multitaper And Conventional Univariate Techniques. 561 pp.,Cambridge Univ. Press, New York, 1993.

Russell III, J.M., Mlynczak, M.G., Gordley, L.L., Tansock, Jr., J.J., Esplin, R.W., 1999. Overview of the SABER experiment and preliminary calibration results. SPIE's Int. Symp.

Opt. Sci. Eng. Instrum. 277–288. https://doi.org/10.1117/12.366382

Sato, K., Yamada, M., 2004. Vertical structure of atmospheric gravity waves revealed by the wavelet analysis. J. Geophys. Res. 99, 20623. https://doi.org/10.1029/94jd01818

Sharma, S., Kumar, P., Vaishnav, R., Jethva, C., Beig, G., 2017. A study of the middle atmospheric thermal structure over western India: Satellite data and comparisons with models. Adv. Sp. Res. 60, 2402–2413. https://doi.org/10.1016/j.asr.2017.09.021

Siva Kumar, V., P. B. Rao, and M. Krishnaiah, 2003. Lidar measurements of stratosphere-mesosphere thermal structure at a low latitude: Comparison with satellite data and models, J. Geophys. Res., 108(D11), 4342, https://doi.org/10.1029/2002JD003029.

Smith, S.A., Fritts, D.C., Vanzandt, T.E., 1987. Evidence for a Saturated Spectrum of Atmospheric Gravity Waves. J. Atmos. Sci. 44, 1404–1410. https://doi.org/10.1175/1520-0469(1987)044<1404:EFASSO>2.0.CO;2

Tsuda, T., Vanzandt, E, Mizumoto, M., Kato, S., Fukao, S., 1991. Spectral Analysis of Temperature and Brunt-Väisälä Frequency Fluctuations Observed by Radiosondes. J. Geophys. Res. Atmos. 96, 17265–17278. https://doi.org/10.1029/91JD01944

Tsuda, T., Hocke, K., 2002. Vertical Wave Number Spectrum of Temperature Fluctuations in the Stratosphere using GPS Occultation Data. J. Meteorol. Soc. Japan 80, 925–938. https://doi.org/10.2151/jmsj.80.925

Tsuda, T., Inoue, T., Fritts, D.C., VanZandt, T.E., Kato, S., Sato, T., Fukao, S., 1989. MST Rader Observations of a Saturated Gravity Wave Spectrum. J. Atmos. Sci., 46, 2440–2447, https://doi.org/10.1175/1520-0469(1989)046<2440:MROOAS>2.0.CO;2

VanZandt, T.E., 1982. A universal spectrum of buoyancy waves in the atmosphere. Geophys. Res. Lett. 9, 575–578. https://doi.org/10.1029/GL009i005p00575

Wu, Yong-fu and Widdel, H.-U., 1989. Observational evidence of a saturated gravity wave spectrum in the mesosphere. J. Atmos. Terr. PhysicsTerrestrial Phys. 51, 991–996. https://doi.org/10.1016/0021-9169(89)90014-7

Yan, Y.Y., Zhang, S.D., Huang, C.M., Huang, K.M., Gong, Y., Gan, Q., 2019. The vertical wave number spectra of potential energy density in the stratosphere deduced from the COSMIC satellite observation. Q. J. R. Meteorol. Soc. 145, 318–336. https://doi.org/10.1002/qj.3433

Yu, C., Yi, F., 2008. Atmospheric temperature profiling by joint Raman, Rayleigh and Fe Boltzmann lidar measurements. J. Atmos. Solar-Terrestrial Phys. 70, 1281–1288. https://doi.org/10.1016/j.jastp.2008.04.002

Zhang, S.D., Huang, C.M., Huang, K.M., Gong, Y., Chen, G., Gan, Q., Zhang, Y.H., 2017a. Latitudinal and Seasonal Variations of Vertical Wave Number Spectra of Three-Dimensional Winds Revealed by Radiosonde Observations. J. Geophys. Res. Atmos. 122, 13,174-13,190. https://doi.org/10.1002/2017JD027602

Zhang, S. D., Ming Huang, C., Ming Huang, K., Hui Zhang, Y., Gong, Y., Gan, Q., 2017b. Vertical wavenumber spectra of three-dimensional winds revealed by radiosonde observations at midlatitude. Ann. Geophys. 35, 107–116. https://doi.org/10.5194/angeo-35-

107-2017

Figure Captions

Figure 1. Altitude profile (33-70 km) of vertical wavenumber spectra of Rayleigh lidar temperature during 14-17 March 2004 over Mt. Abu (24.5º N, 72.7º E) [14 March: a-d; 15 March: e-h; 16 March: i-l; 17 March: m-p]. The slope lines and values are calculated considering both without and with 'prewhitening/postcoloring' technique where the first slope region (Slope 1; denoted with magenta color) indicates slope value without 'prewhitening/postcoloring' and the second slope region (Slope 2; denoted with blue color) indicates slope value with 'prewhitening/postcoloring'.

Figure 2. Same as Figure 1 except for during 18-21 March 2004 [18 March: a-d; 19 March: e-h; 20 March: i-l; 21 March: m-p].

Figure 3. Altitude profile (30-66 km) of vertical wavenumber spectra of Rayleigh lidar temperature during 19-22 March 2004 over Gadanki (13.5º N, 79.2º E) [19 March: a-d; 20 March: e-h; 21 March: i-l; 22 March: m-p]. The slope lines and values are calculated considering both without and with 'prewhitening/postcoloring' technique where the first slope region (Slope 1; denoted with magenta color) indicates slope value without 'prewhitening/postcoloring' and the second slope region (Slope 2; denoted with blue color) indicates slope value with 'prewhitening/postcoloring'.

Figure 4. Same as Figure 3 except for during 23-26 March 2004 [23 March: a-d; 24 March: e-h; 25 March: i-l; 26 March: m-p].

Figure 5. Comparison of vertical wavenumber spectra of height profile of Rayleigh lidar temperature over Mt. Abu [33-40 km (d); 40-50 km (c); 50-60 km (b); 60-70 km (a)] and Gadanki [30-40 km (h); 40-50 km (g); 50-60 km (f); 60-66 km (e)] on 19 March 2004 [Slope 1 (denoted with magenta color) indicates slope value without 'prewhitening/postcoloring' and Slope 2 (denoted with blue color) indicates slope value with 'prewhitening/postcoloring'].

Figure 6. Same as Figure 5 except for on 20 March 2004.

Figure 7. Same as Figure 5 except for on 21 March 2004.

Figure 8. Comparison of altitude profile (30-70 km) of vertical wavenumber spectra of SABER temperature on 18 March 2004 over Mt. Abu [30-40 km (d); 40-50 km (c); 50-60 km (b); 60-70 km (a)] and 19 March 2004 over Gadanki [30-40 km (h); 40-50 km (g); 50-60 km (f); 60-70 km (e)]. Slope value without 'prewhitening/postcoloring' is represented as Slope 1 (with magenta color) and with 'prewhitening/postcoloring' as Slope 2 (with blue color).

Figure 9. Same as Figure 8 except for 21 March 2004 over Mt. Abu and 20 March 2004 over Gadanki.

Figure 10. Height profile of amplitude and phase of wave oscillations in Rayleigh lidar temperature over Gadanki (during 19-26 March 2004; top panel) and Mt. Abu (during 14-21 March 2004; lower panel). The dominant oscillations observed are shown in different colors (blue color: 4-day oscillation, green color: 2.7-day oscillation and wine color: 2-day oscillation).

Table Captions

Table 1. Vertical wavenumber (VWN) spectral slope (approximate values) using lidar observations without Pre-whitening and Post-Coloring (PWPC)] and with PWPC over: A) Mt. Abu (24.5º N, 72.7º E), and B) Gadanki (13.5º N, 79.2º E). The spectral slopes in bracket indicates VWN spectral slope with PWPC.

Table 2. Co-efficient of determination (R^2) of vertical wavenumber spectral slopes using lidar observation [with and without Pre-whitening and Post-Coloring (PWPC)] over: A) Mount Abu (24.5º N, 72.7º E), and B) Gadanki (13.5º N, 79.2º E). The values denoted with '±' sign are standard deviation of R^2.

Table 3. (i) Vertical wavenumber (VWN) spectral slope (approximate values) without and with Pre-whitening and Post-Coloring (PWPC)], (ii) Co-efficient of determination (R^2) obtained using SABER/TIMED observations without and with Pre-whitening and Post-Coloring (PWPC)] over Mt. Abu (24.5º N, 72.7º E) on 18 and 21 March 2004 and Gadanki (13.5º N, 79.2º E) on 19 and 20 March 2004. The spectral slopes in bracket indicates VWN spectral slope and Co-efficient of determination (R^2) with PWPC.

Table 1. Vertical wavenumber (VWN) spectral slope (approximate values) using lidar observations without Pre-whitening and Post-Coloring (PWPC)] and with PWPC over: A) Mt. Abu (24.5º N, 72.7º E), and B) Gadanki (13.5º N, 79.2º E). The spectral slopes in bracket indicates VWN spectral slope with PWPC.

A) Mount Abu (24.5º N, 72.7º E)								
Altitude Range (km)	**14 March**	**15 March**	**16 March**	**17 March**	**18 March**	**19 March**	**20 March**	**21 March**
33-40	-2.63 (-2.81)	-2.57 (-2.78)	-2.68 (-2.84)	-2.64 (-2.81)	-2.66 (-2.82)	-2.73 (-2.86)	-2.61 (-2.80)	-2.68 (-2.83)
40-50	-2.82 (-2.91)	-2.67 (-2.83)	-2.77 (-2.88)	-2.80 (-2.90)	-2.50 (-2.75)	-2.94 (-2.97)	-2.86 (-2.93)	-2.93 (-2.96)
50-60	-2.46 (-2.73)	-2.43 (-2.71)	-2.88 (-2.94)	-2.14 (-2.57)	-2.79 (-2.89)	-2.42 (-2.71)	-2.66 (-2.83)	-2.52 (-2.76)
60-70	-2.72 (-2.86)	-2.65 (-2.82)	-2.72 (-2.83)	-2.58 (-2.79)	-2.75 (-2.87)	-2.68 (-2.84)	-2.75 (-2.81)	-2.79 (-2.89)

B) Gadanki (13.5º N, 79.2º E)								
Altitude Range (km)	**19 March**	**20 March**	**21 March**	**22 March**	**23 March**	**24 March**	**25 March**	**26 March**
30-40	-2.94 (-2.97)	-2.71 (-2.86)	-2.83 (-2.91)	-3.01 (-3.00)	-2.71 (-2.86)	-2.86 (-2.93)	-2.69 (-2.84)	-2.50 (-2.75)
40-50	-2.94 (-2.97)	-3.01 (-3.01)	-2.99 (-2.99)	-3.25 (-3.13)	-2.94 (-2.97)	-2.82 (-2.90)	-3.17 (-3.09)	-2.78 (-2.89)
50-60	-2.86 (-2.93)	-2.53 (-2.76)	-2.93 (-2.96)	-2.68 (-2.84)	-2.56 (-2.78)	-2.40 (-2.70)	-2.47 (-2.73)	-2.74 (-2.87)
60-66	-2.31 (-2.65)	-2.40 (-2.70)	-2.31 (-2.58)	-2.30 (-2.65)	-1.78 (-2.39)	-2.70 (-2.85)	-1.78 (-2.90)	-2.36 (-2.68)

Table 2. Co-efficient of determination (R^2) of vertical wavenumber spectral slopes using lidar observation [with and without Pre-whitening and Post-Coloring (PWPC)] over: A) Mount Abu (24.5º N, 72.7º E), and B) Gadanki (13.5º N, 79.2º E). The values denoted with '±' sign are standard deviation of R^2.

A) Mount Abu (24.5º N, 72.7º E)								
i) Co-efficient of determination (R^2) [without Pre-whitening and Post-Coloring (PWPC)]								
Altitude Range (km)	**14 March**	**15 March**	**16 March**	**17 March**	**18 March**	**19 March**	**20 March**	**21 March**
33-40	0.995 ± 0.01	0.998 ± 0.01	0.987 ± 0.01	0.994 ± 0.02	0.995 ± 0.01	0.992 ± 0.01	0.996 ± 0.01	0.996 ± 0.03
40-50	0.982 ± 0.01	0.986 ± 0.01	0.975 ± 0.01	0.989 ± 0.02	0.976 ± 0.01	0.984 ± 0.01	0.968 ± 0.01	0.989 ± 0.03
50-60	0.984 ± 0.01	0.982 ± 0.01	0.972 ± 0.01	0.952 ± 0.02	0.967 ± 0.01	0.980 ± 0.01	0.988 ± 0.01	0.935 ± 0.03
60-70	0.967 ± 0.01	0.979 ± 0.01	0.967 ± 0.01	0.987 ± 0.02	0.974 ± 0.01	0.996 ± 0.01	0.974 ± 0.01	0.998 ± 0.03
ii) Co-efficient of determination (R^2) [with Pre-whitening and Post-Coloring (PWPC)]								
Altitude Range (km)	**14 March**	**15 March**	**16 March**	**17 March**	**18 March**	**19 March**	**20 March**	**21 March**
33-40	0.999 ± 0.00	1.00 ± 0.00	0.997 ± 0.00	0.999 ± 0.00	0.999 ± 0.00	0.998 ± 0.00	0.999 ± 0.00	0.999 ± 0.01
40-50	0.996 ± 0.00	0.997 ± 0.00	0.994 ± 0.00	0.997 ± 0.00	0.995 ± 0.00	0.996 ± 0.00	0.992 ± 0.00	0.997 ± 0.01
50-60	0.997 ± 0.00	0.996 ± 0.00	0.993 ± 0.00	0.991 ± 0.00	0.992 ± 0.00	0.996 ± 0.00	0.997 ± 0.00	0.986 ± 0.01
60-70	0.992 ± 0.00	0.995 ± 0.00	0.991 ± 0.00	0.997 ± 0.00	0.994 ± 0.00	0.999 ± 0.00	0.996 ± 0.00	0.999 ± 0.01
B) Gadanki (13.5º N, 79.2º E)								
i) Co-efficient of determination (R^2) [without Pre-whitening and Post-Coloring (PWPC)]								
Altitude Range (km)	**19 March**	**20 March**	**21 March**	**22 March**	**23 March**	**24 March**	**25 March**	**26 March**
30-40	0.904 ± 0.03	0.865 ± 0.09	0.973 ± 0.09	0.956 ± 0.13	0.973 ± 0.18	0.976 ± 0.14	0.976 ± 0.16	0.888 ± 0.04
40-50	0.948 ± 0.03	0.957 ± 0.09	0.778 ± 0.09	0.949 ± 0.13	0.931 ± 0.18	0.783 ± 0.14	0.809 ± 0.16	0.912 ± 0.04
50-60	0.882 ± 0.03	0.751 ± 0.09	0.794 ± 0.09	0.672 ± 0.13	0.882 ± 0.18	0.817 ± 0.14	0.812 ± 0.16	0.898 ± 0.04

60-66	0.905 ± 0.03	0.802 ± 0.09	0.905 ± 0.09	0.812 ± 0.13	0.582 ± 0.18	0.632 ± 0.14	0.582 ± 0.16	0.825 ± 0.04
ii) Co-efficient of determination (R^2) [with Pre-whitening and Post-Coloring (PWPC)]								
Altitude Range (km)	**19 March**	**20 March**	**21 March**	**22 March**	**23 March**	**24 March**	**25 March**	**26 March**
30-40	0.975 ± 0.01	0.966 ± 0.02	0.994 ± 0.03	0.989 ± 0.04	0.994 ± 0.04	0.994 ± 0.05	0.994 ± 0.02	0.975 ± 0.01
40-50	0.987 ± 0.01	0.989 ± 0.02	0.934 ± 0.03	0.986 ± 0.04	0.982 ± 0.04	0.939 ± 0.05	0.941 ± 0.02	0.978± 0.01
50-60	0.969 ± 0.01	0.935 ± 0.02	0.940 ± 0.03	0.902 ± 0.04	0.972 ± 0.04	0.957 ± 0.05	0.955 ± 0.02	0.975 ± 0.01
60-66	0.980 ± 0.01	0.953 ± 0.02	0.938 ± 0.03	0.958 ± 0.04	0.909 ± 0.04	0.884 ± 0.05	0.976 ± 0.02	0.960 ± 0.01

Table 3. (i) Vertical wavenumber (VWN) spectral slope (approximate values) without and with Pre-whitening and Post-Coloring (PWPC)], (ii) Co-efficient of determination (R^2) obtained using SABER/TIMED observations without and with Pre-whitening and Post-Coloring (PWPC)] over Mt. Abu (24.5º N, 72.7º E) on 18 and 21 March 2004 and Gadanki (13.5º N, 79.2º E) on 19 and 20 March 2004. The spectral slopes in bracket indicates VWN spectral slope and Co-efficient of determination (R^2) with PWPC.

i) Vertical wavenumber (VWN) spectral slope (approximate values)				
Altitude Range (km)	**18 March (Mt. Abu)**	**19 March (Gadanki)**	**21 March (Mt. Abu)**	**20 March (Gadanki)**
30-40	-2.61 (-2.79)	-2.70 (-2.84)	-2.49 (-2.73)	-2.30 (-2.64)
40-50	-6.97 (-4.97)	-0.09 (-1.53)	-2.60 (-2.78)	-2.75 (-2.86)
50-60	-2.34 (-2.66)	-2.97 (-2.97)	-2.82 (-2.90)	-2.36 (-2.67)
60-70	-2.43 (-2.70)	-2.63 (-2.80)	-2.19 (-2.58)	-2.71 (-2.84)
ii) Co-efficient of determination (R^2)				
Altitude Range (km)	**18 March (Mt. Abu)**	**19 March (Gadanki)**	**21 March (Mt. Abu)**	**20 March (Gadanki)**
30-40	0.998 ± 0.04 (0.999 ± 0.02)	0.987 ± 0.49 (0.997 ± 0.17)	0.992 ± 0.01 (0.998 ± 0.00)	0.993 ± 0.00 (0.998 ± 0.00)
40-50	0.907 ± 0.04 (0.952 ± 0.02)	0.175 ± 0.49 (0.656 ± 0.17)	0.989 ± 0.01 (0.997 ± 0.00)	0.992 ± 0.00 (0.998 ± 0.00)
50-60	0.949 ± 0.04 (0.989 ± 0.02)	0.974 ± 0.49 (0.993 ± 0.17)	0.978 ± 0.01 (0.994 ± 0.00)	0.983 ± 0.00 (0.996 ± 0.00)
60-70	0.985 ± 0.04 (0.997 ± 0.02)	0.998 ± 0.49 (0.999 ± 0.17)	0.996 ± 0.01 (0.999 ± 0.00)	0.993 ± 0.00 (0.998 ± 0.00)

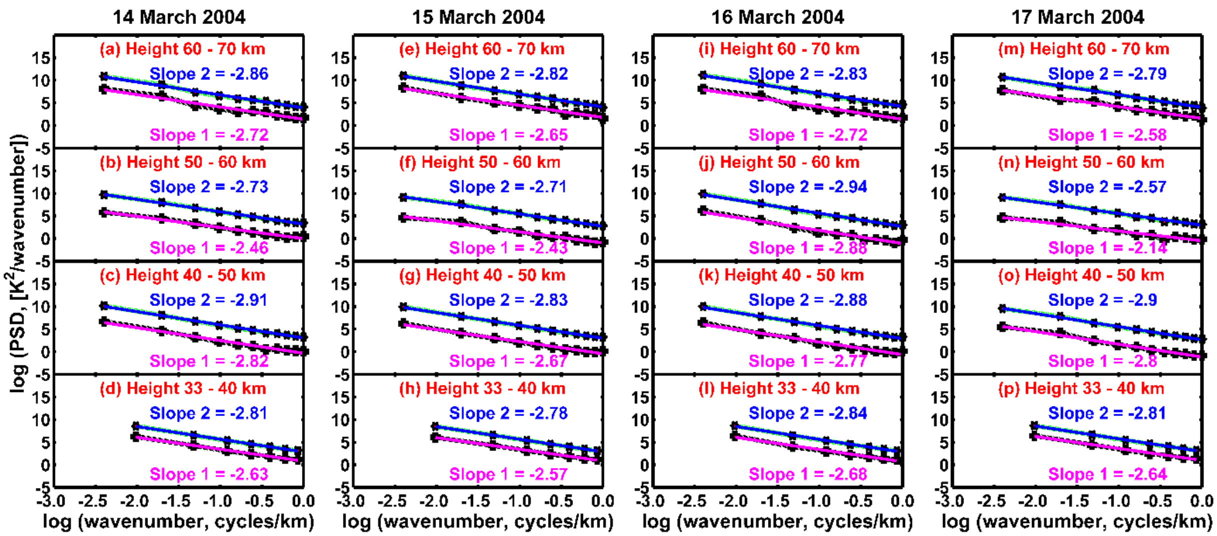

Figure 1. Altitude profile (33-70 km) of vertical wavenumber spectra of Rayleigh lidar temperature during 14-17 March 2004 over Mt. Abu (24.5º N, 72.7º E) [14 March: a-d; 15 March: e-h; 16 March: i-l; 17 March: m-p]. The slope lines and values are calculated considering both without and with ‘prewhitening/postcoloring’ technique where the first slope region (Slope 1; denoted with magenta color) indicates slope value without ‘prewhitening/postcoloring’ and the second slope region (Slope 2; denoted with blue color) indicates slope value with ‘prewhitening/postcoloring’.

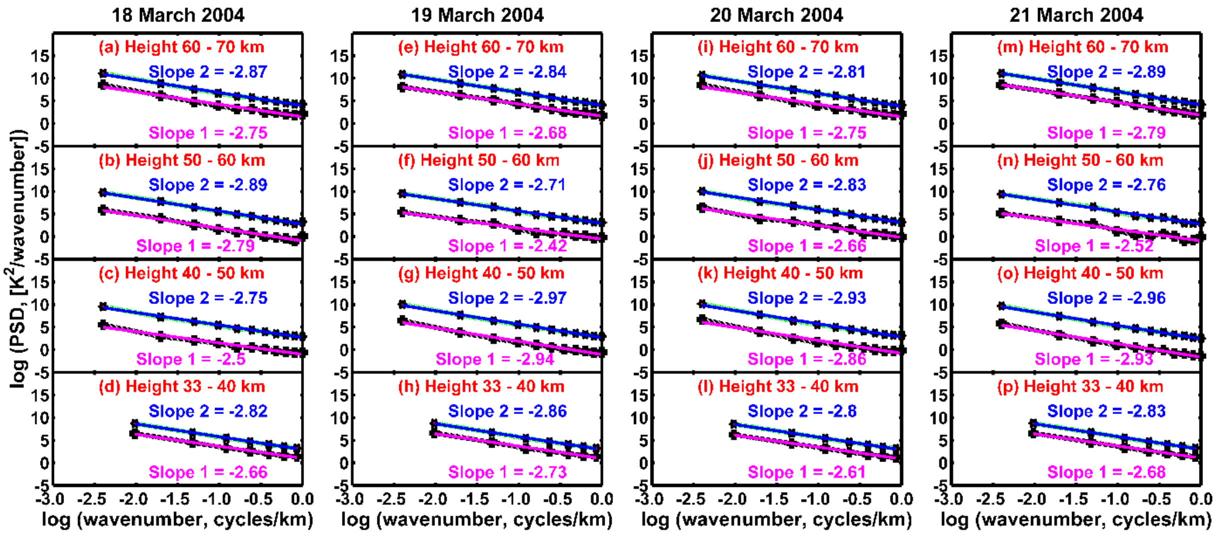

Figure 2. Same as Figure 1 except for during 18-21 March 2004 [18 March: a-d; 19 March: e-h; 20 March: i-l; 21 March: m-p].

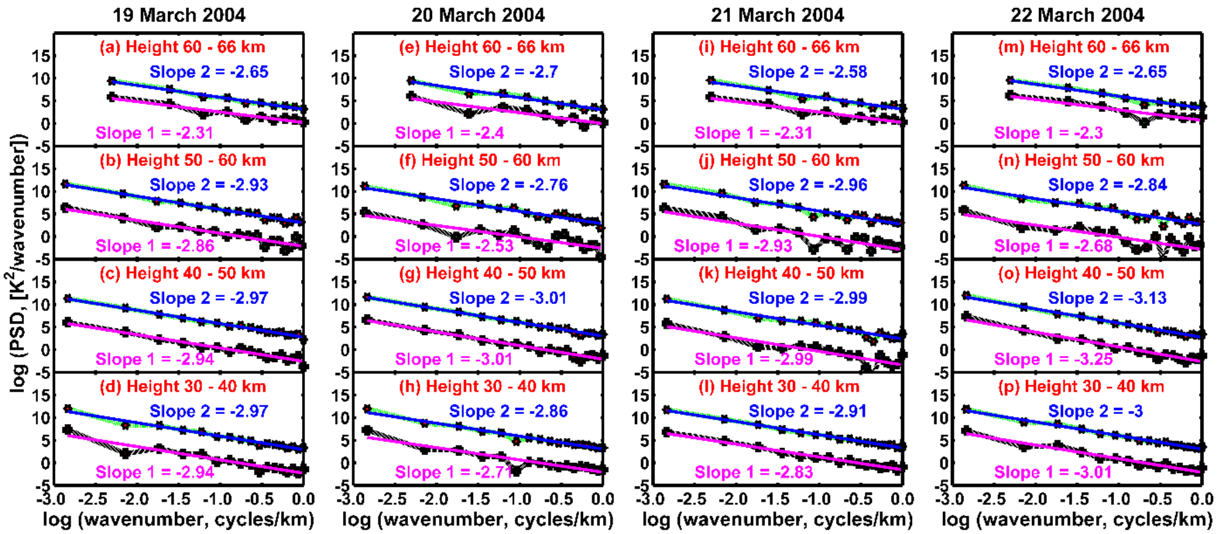

Figure 3. Altitude profile (30-66 km) of vertical wavenumber spectra of Rayleigh lidar temperature during 19-22 March 2004 over Gadanki (13.5º N, 79.2º E). [19 March: a-d; 20 March: e-h; 21 March: i-l; 22 March: m-p]. The slope lines and values are calculated considering both without and with 'prewhitening/postcoloring' technique where the first slope region (Slope 1; denoted with magenta color) indicates slope value without 'prewhitening/postcoloring' and the second slope region (Slope 2; denoted with blue color) indicates slope value with 'prewhitening/postcoloring'.

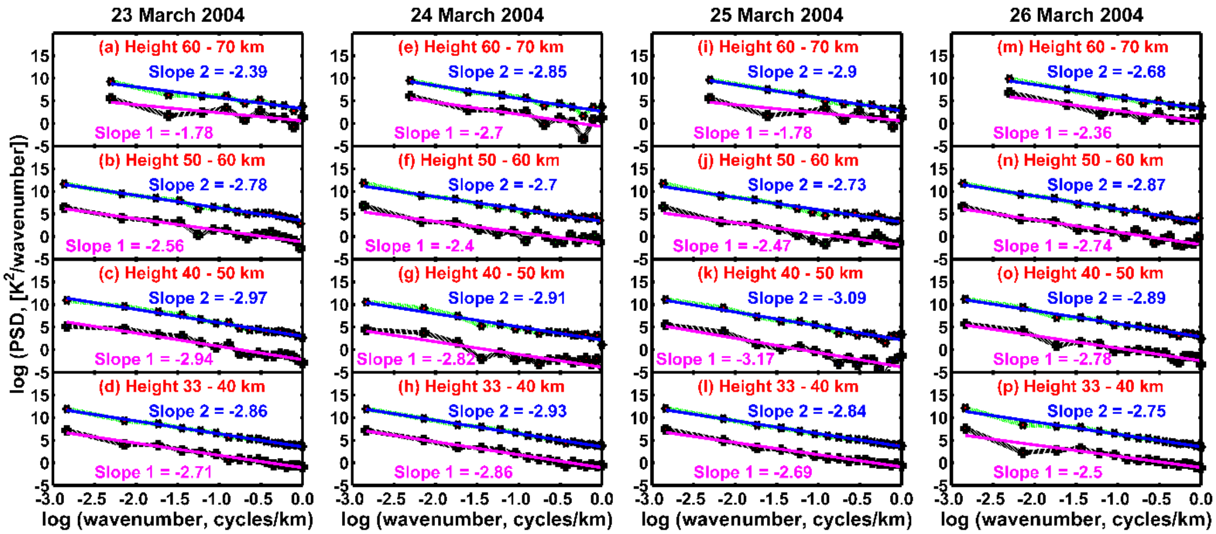

Figure 4. Same as Figure 3 except for during 23-26 March 2004 [23 March: a-d; 24 March: e-h; 25 March: i-l; 26 March: m-p].

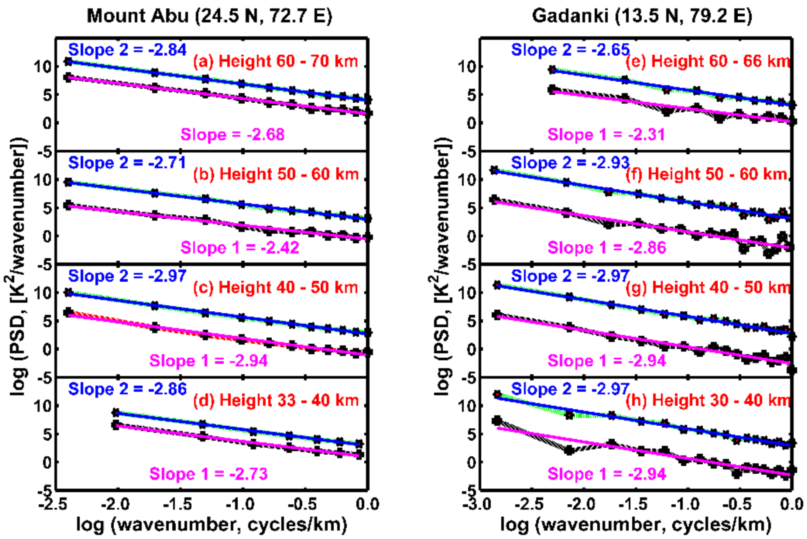

Figure 5. Comparison of vertical wavenumber spectra of height profile of Rayleigh lidar temperature over Mt. Abu [33-40 km (d); 40-50 km (c); 50-60 km (b); 60-70 km (a)] and Gadanki [30-40 km (h); 40-50 km (g); 50-60 km (f); 60-66 km (e)] on 19 March 2004 [Slope 1 (denoted with magenta color) indicates slope value without ‘prewhitening/postcoloring’ and Slope 2 (denoted with blue color) indicates slope value with ‘prewhitening/postcoloring’].

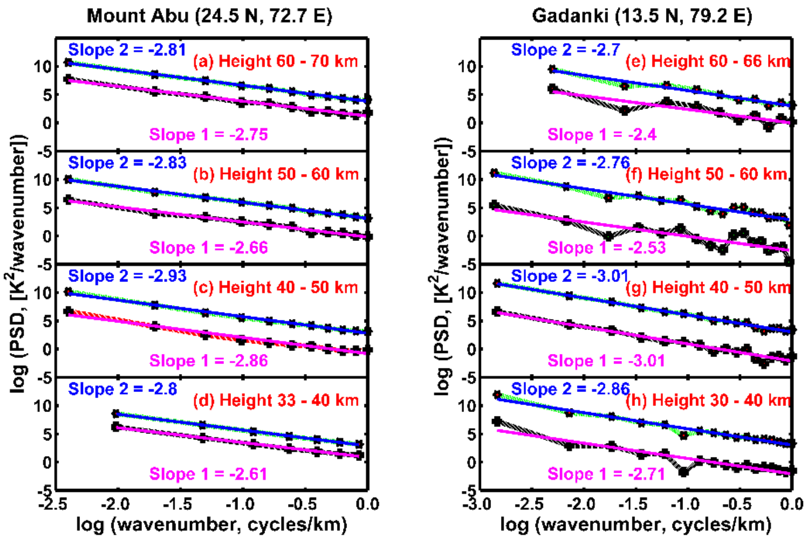

Figure 6. Same as Figure 5 except for on 20 March 2004.

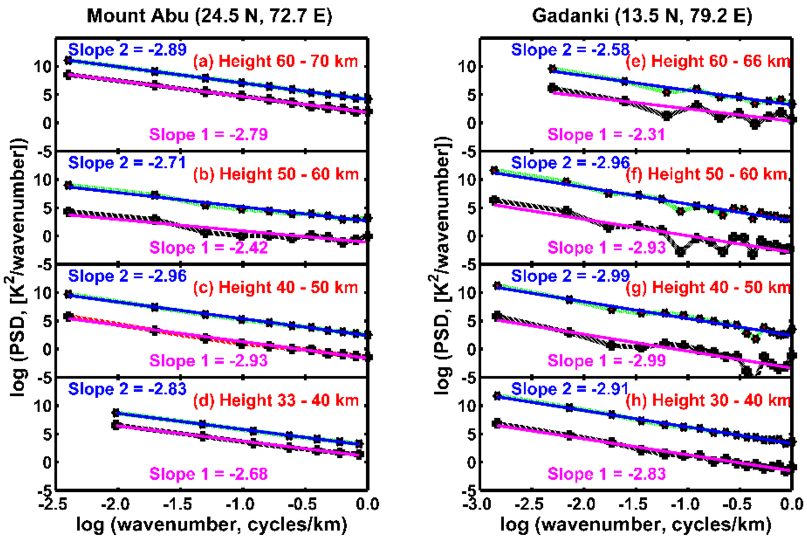

Figure 7. Same as Figure 5 except for on 21 March 2004.

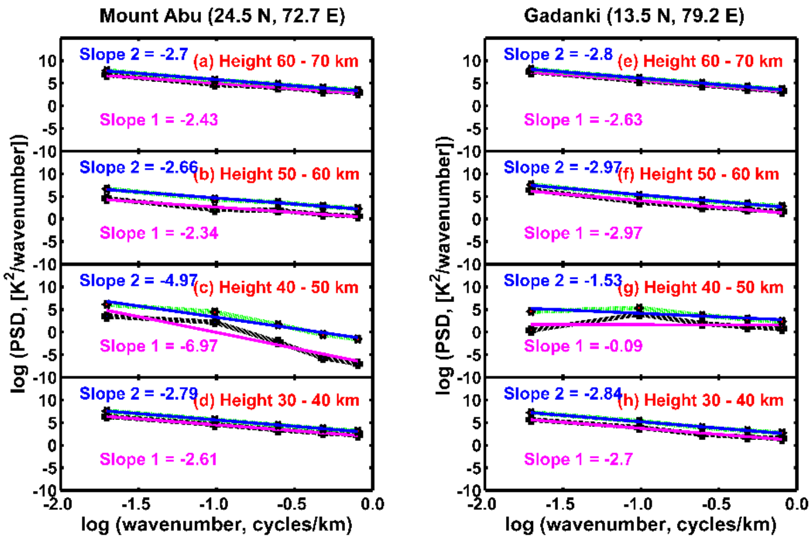

Figure 8. Comparison of altitude profile (30-70 km) of vertical wavenumber spectra of SABER temperature on 18 March 2004 over Mt. Abu [30-40 km (d); 40-50 km (c); 50-60 km (b); 60-70 km (a)] and 19 March 2004 over Gadanki [30-40 km (h); 40-50 km (g); 50-60 km (f); 60-70 km (e)]. Slope value without 'prewhitening/postcoloring' is represented as Slope 1 (with magenta color) and with 'prewhitening/postcoloring' as Slope 2 (with blue color).

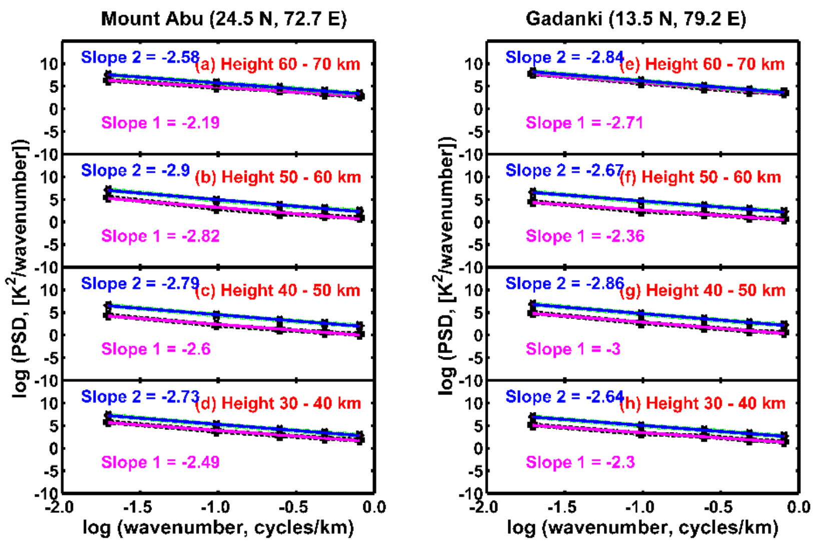

Figure 9. Same as Figure 8 except for 21 March 2004 over Mt. Abu and 20 March 2004 over Gadanki.

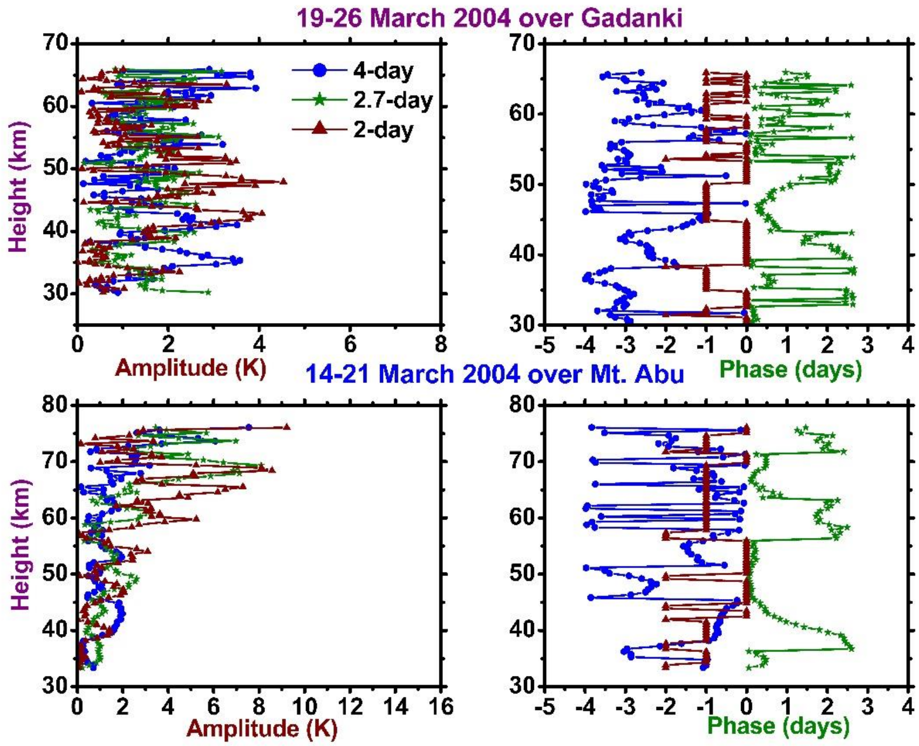

Figure 10. Height profile of amplitude and phase of wave oscillations in Rayleigh lidar temperature over Gadanki (during 19-26 March 2004; top panel) and Mt. Abu (during 14-21 March 2004; lower panel). The dominant oscillations observed are shown in different colors (blue color: 4-day oscillation, green color: 2.7-day oscillation and wine color: 2-day oscillation).